PAGEOPH, Vol. 137, No. 4 (1991) 0033–4553/91/040409–11$1.50 + 0.20/0

A Note on the Stress-Dilatancy Relation for Simulated Fault Gouge

CHRIS MARONE[1]

Abstract—Theoretical constraints on the stress-dilation relation for a deforming Coulomb material require $\nu \leq \theta$ if $C = 0$ and $\nu \leq \sin^{-1}(\tau_m/\sigma_m)$ always, where ν is the dilation angle, θ is the friction angle, C is cohesion, τ_m is the maximum shear stress, and σ_m is the mean effective stress. Recent laboratory measurements of friction and dilatancy of simulated fault gouge show that small amplitude shear-load cycling causes compaction and consolidation. Comparison of the data with theory indicates that such load cycling produces: (1) increased coefficient of friction (or friction angle), (2) increased cohesion, and (3) increased dilatancy rate (or dilation angle). Under certain conditions of load cycling without significant plastic shear strain accumulation ($\gamma^p < 0.005$) we find that ν exceeds both θ and, in contrast to theory, $\sin^{-1}(\tau_m/\sigma_m)$. This result is interpreted in terms of enhanced cohesion and overconsolidation, which lead to residual stresses within the gouge. An analogy is drawn between these special loading conditions and those extant on natural faults. In particular, our results imply that jostling and minor stress variations associated with microearthquakes may produce strengthening of fault gouge and changes in the fault zone's stress-dilatancy relation. Hence, compaction associated with microseismicity may lead to subsequent dilation of fault gouge, even for faults with large displacement rates and large net offsets (e.g., San Andreas). In regions where such dilation persists over sufficient displacements (on the order of the critical slip distance for seismic faulting) it may tend to inhibit unstable slip.

Key words: Fault gouge, dilatancy, shear localization, friction, Coulomb failure, mechanical healing.

Introduction

The stress-dilatancy relation for fault gouge has long been the subject of considerable interest, not least because of its relevance to the problems of shear localization, the onset of instability (e.g., MEAD, 1925; FRANK, 1965; RUDNICKI and RICE, 1975; HOBBS *et al.*, 1991), and earthquake prediction (e.g., SCHOLZ *et al.*, 1973). Models for shear localization and instability generally require specific stress-strain-dilatancy relationships [e.g., that $d^2\phi/d\gamma^2$ become negative at the peak stress, where ϕ is porosity and γ is shear strain (FRANK, 1965)] and thus application

[1] Seismographic Station and Department of Geology and Geophysics, University of California, Berkeley, CA 94720, U.S.A.

of the models requires knowledge of relevant stress-dilatancy relations. However, detailed experimental measurements at pressures appropriate to seismogenic conditions are sparse. For example, RUDNICKI and RICE (1975) showed that under certain conditions shear localization and potential instability is possible during overall hardening of the stress-strain curve, however, data appropriate to test their theory have only recently become available (ORD *et al.*, 1991).

MARONE *et al.* (1990) report experimental measurements of the stress-dilatancy relationship in simulated fault gouge. Their work shows a link between dilatancy within gouge and the second-order friction terms that appear in the rate and state variable constitutive laws of DIETERICH (1978, 1981) and RUINA (1983). The friction constitutive laws have been found to describe both laboratory friction data and observations of natural faults (for recent reviews see, RUDNICKI, 1988; TULLIS, 1988; SCHOLZ, 1990). The work of MARONE *et al.* (1990) indicates that gouge exhibits velocity strengthening frictional behavior (increased friction with slip velocity) during at least a portion of its strain history and that velocity strengthening is the result of changes in the dilatancy rate. Because velocity strengthening implies inherently stable sliding (e.g.. GU *et al.*, 1984) their results highlight the importance of understanding the relationship between volume change and frictional strength of fault gouge.

In this paper we compare a theoretical constraint on the stress-dilatancy relation with experimental data and show that consolidation associated with cyclic shear loading results in both increased friction and cohesion. The paper begins with a brief summary of the theory, after which we present and evaluate experimental data in light of the theoretical constraint.

Stress-Dilatancy Relation: Theoretical

Two aspects of the stress-dilatancy relation are particularly important for modeling shear localization, instability, and earthquake precursory phenomena: (1) the onset of dilatancy relative to features in the stress-strain curve (e.g., the peak stress or ultimate strength), and (2) the relative magnitudes of the dilatancy rate (or dilatancy angle v, defined below) and friction angle θ ($\theta = \tan^{-1} \mu^i$, where μ^i is the coefficient of internal friction). Although the theoretical constraint $v < \theta$ for cohesionless materials is well known in soil mechanics (e.g., VERMEER and DE BORST, 1984) it has received little attention in the geophysical literature. For this reason, and to clarify the relationship between friction and dilation angles and parameters such as the coefficient of sliding friction μ, we provide the following brief analysis.

If we assume plane strain deformation within a thin layer of sand or granular fault gouge, the rate of work per unit volume ($\dot{w}$) during deformation is

$$\dot{w} = \sigma_1 \dot{\varepsilon}_1 + \sigma_2 \dot{\varepsilon}_2, \tag{1}$$

where σ_1, σ_2 are the principal stresses and $\dot{\varepsilon}_1, \dot{\varepsilon}_2$ are the principal strain rates (compression taken positive). We may define the dilation angle (v) as

$$\sin v = -\frac{(\dot{\varepsilon}_1 + \dot{\varepsilon}_2)}{|\dot{\varepsilon}_1 - \dot{\varepsilon}_2|} \tag{2}$$

which is consistent with the definition $\sin v = d\varepsilon_v^p / d\gamma^p$: the dilation angle represents the ratio of (plastic) volumetric to shear strain increments (RUDNICKI and RICE, 1975) if elastic deformations are neglected. If we assume $\dot{\varepsilon}_1 > \dot{\varepsilon}_2$, substitution of equation (2) into (1) yields a relation for $\dot{w}$ in terms of the stress difference, the dilation angle, the mean effective stress (total stress minus pore pressure), and the differential strain rate:

$$\dot{w} = \left\{\frac{(\sigma_1 - \sigma_2)}{2} - \sin v \frac{(\sigma_1 + \sigma_2)}{2}\right\}(\dot{\varepsilon}_1 - \dot{\varepsilon}_2). \tag{3}$$

We may then write the Coulomb failure criteria:

$$\frac{(\sigma_1 - \sigma_2)}{2} - \sin\theta \frac{(\sigma_1 + \sigma_2)}{2} - C\cos\theta = 0, \tag{4}$$

where θ is the friction angle and C is cohesion. Substituting equation (4) into (3) yields a relation, in terms of friction and dilation angle, for the rate of work during deformation of a Coulomb material:

$$\dot{w} = \left\{\frac{(\sigma_1 + \sigma_2)}{2}(\sin\theta - \sin v) + C\cos\theta\right\}(\dot{\varepsilon}_1 - \dot{\varepsilon}_2). \tag{5}$$

Since $\dot{w}$ must be positive or zero, we have:

$$\frac{(\sigma_1 + \sigma_2)}{2}(\sin\theta - \sin v) + C\cos\theta \geq 0, \tag{6}$$

indicating that the dilation angle cannot exceed the friction angle for a cohesionless material. For a material with $C \neq 0$, v may exceed θ as indicated in equation (6).

Recognizing that the experimental friction data considered below are reported in terms of the effective normal stress (total stress minus pore pressure) $\sigma_n = (\sigma_1 + \sigma_2)/2$, shear stress $\tau = \tau_m = (\sigma_1 - \sigma_2)/2$ [the gouge layer is at 45° to σ_1], and their ratio $\mu = \tau/\sigma_n$, the above may be recast to yield a relationship between the dilation angle and τ/σ_n. Using these parameters, equation (6) becomes:

$$\sin v \leq \frac{C\cos\theta}{\sigma_n} + \sin\theta. \tag{7}$$

The Coulomb relation in terms of τ_m, θ, and the mean effective stress (which in a thin layer is equivalent to σ_n) is:

$$\frac{\tau_m}{\sigma_m} = \frac{\tau}{\sigma_n} = \frac{C\cos\theta}{\sigma_n} + \sin\theta, \tag{8}$$

which upon substitution of (7) into (8) yields:

$$\sin \nu \leq \frac{\tau}{\sigma_n}. \tag{9}$$

The inequalities expressed in (6) and (9) have a number of interesting consequences. In particular, the basis of the "normality rule" of classical plasticity is the equality of ν and θ (for further discussion see, for example, RUDNICKI and RICE, 1975; VERMEER and DE BORST 1984; HOBBS *et al.*, 1991). Although experimental data for soils and rocks indicate that normality does not hold in general, existing measurements show only the case $\nu \leq \theta$ in agreement with equation (6). We show here a situation for which ν exceeds both θ and $\sin^{-1}(\tau/\sigma_n)$. The data are interpreted in terms of overconsolidation and residual stresses caused by cyclic loading and an analogy is drawn between these special loading conditions and those of natural faults.

Stress-Dilatancy Relation: Experimental

The data presented below are derived from a suite of experiments described in detail by MARONE *et al.* (1990). In those experiments, Ottawa sand (>99% quartz) was used as simulated fault gouge and four-mm thick layers were sheared within steel forcing blocks at 45° to the load axis in a triaxial apparatus. Normal stress across the layer was held constant during shear using a servo-control technique, which involved reducing confining pressure P_c as axial load increased. Drained conditions (pore pressure = 10 MPa) were maintained and volume change was monitored by measuring the fluid flux in or out of the gouge layer. In this paper we confine ourselves to MARONE *et al.*'s experiments at 50–100 MPa effective normal stress. We analyzed ten experiments in detail.

Because normal stress was held constant in the experiments of MARONE *et al.* (1990): (1) porosity changes $d\phi$ are the result of shear stresses/deformation only, and (2) to the extent that bulk dilation of a granular material implies macroscopic relative movement (rolling or sliding) between grains, porosity changes are a measure of the plastic volumetric strain, i.e., $d\phi = d\varepsilon_v^p$. We corrected shear strain measurements for elastic distortion of the experimental sample and apparatus. Thus, after the onset of dilatancy during loading these corrected data represent the plastic shear strain $d\gamma^p$. The dilation angle ν is obtained from $\sin \nu = d\varepsilon_v^p / d\gamma^p$ and it is the latter quantity that is plotted in the figures below. The porosity data were corrected for the effect of offset between the forcing blocks during shear and for volume change at the edge of the layer in association with changes in P_c (see MARONE *et al.*, 1990 for details). These corrections have the effect of reducing by 10–15% the experimentally measured $d\varepsilon_v^p / d\gamma^p$ values.

Data

We present data from two types of experiments: those in which significant plastic strain was imposed prior to unloading (e.g., Figure 2) and those in which the plastic strain increment during a given load cycle was varied (e.g., Figure 3). We begin by showing detailed stress-strain-dilatancy characteristics for the former experiments.

Stress-strain and porosity-strain curves are shown for loading of a gouge layer, which had undergone a shear strain of ≈ 0.77 (Figure 1). The dashed line in Figure 1 indicates the dilatancy rate $d\varepsilon_v^p/d\gamma^p$. Upon loading, the stress-strain curve rose nonlinearly to a peak stress and gradually weakened. Dilatancy began at 10–30% of the peak stress after a small amount of compaction (Figure 1). The dilatancy rate therefore decreased slightly upon loading after which it increased and gradually decayed as the stress-strain curve reached a peak value. The sharp rise in $d\varepsilon_v^p/d\gamma^p$ coincided with the rising position of the stress-strain curve, but $d\varepsilon_v^p/d\gamma^p$ remained less than τ/σ_n. The maximum dilatancy rate was 0.34 ($\nu = 19.9°$), which is 55% of the peak τ/σ_n value.

The overall characteristics of data such as presented in Figure 1 can be summarized as follows (Figure 2). After a period in which shear-load cycling resulted in compaction and strain hardening ($\gamma < 0.4$): (1) dilation occurred during

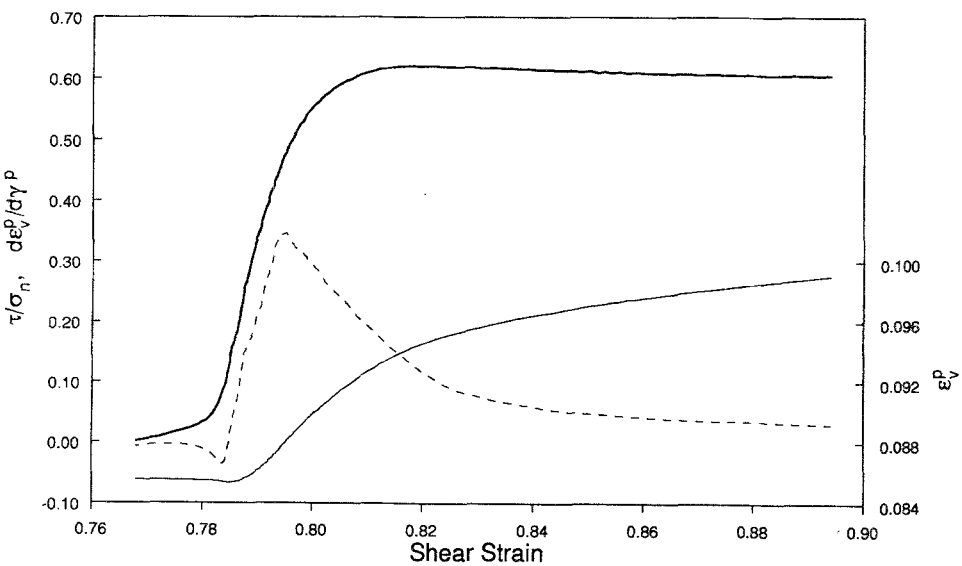

Figure 1

The ratio of shear stress to normal stress τ/σ_n (thick solid line) and plastic volumetric strain ε_v^p (thin solid line) are plotted vs. shear strain γ for a load cycle taken from the experiment shown in Figure 2. Dashed line shows the dilatancy rate $d\varepsilon_v^p/d\gamma^p = \sin\nu$ (plotted on the same scale as τ/σ_n), which was calculated from a linear best fit to a 5-point moving window over the data (each curve represents 140 equally-spaced data points). Note that the dilatancy rate is always less than τ/σ_n.

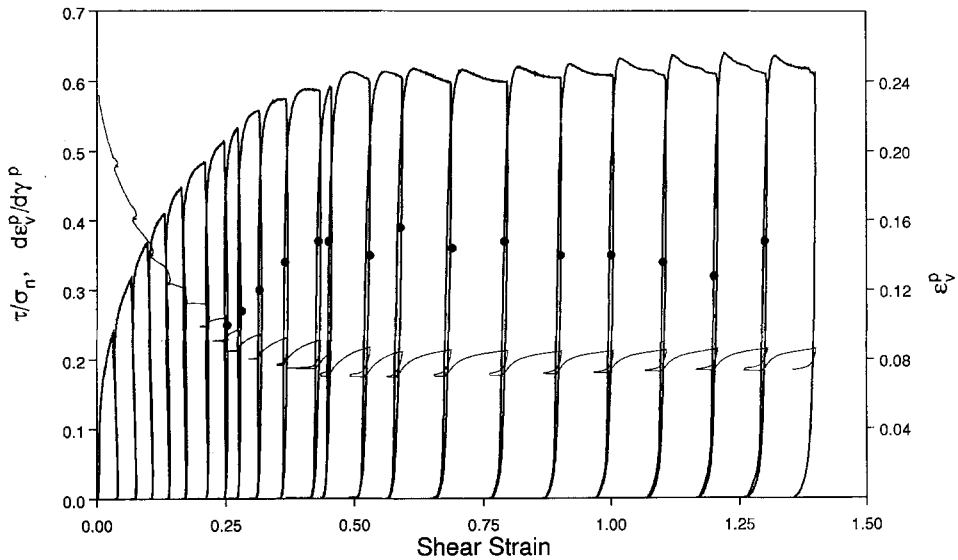

Figure 2

The ratio of shear stress to normal stress τ/σ_n (thick solid line) and plastic volumetric strain ε_v^p (thin solid line) are plotted vs. shear strain γ. Dots indicate maximum dilatancy rate $d\varepsilon_v^p/d\gamma^p$ for a given load cycle (plotted on the same scale as τ/σ_n). Note that the maximum dilatancy rate is always less than the corresponding τ/σ_n value (i.e., the value at an equivalent shear strain) and that the maximum dilatancy rate remains roughly constant independent of total shear strain for $\gamma > \approx 0.4$.

loading (Figure 1), (2) net compaction over a load cycle ceased, and (3) the yield and residual strength reached approximately constant values (Figure 2). The peak magnitude of the dilatancy rate ranged from about 0.3 to 0.4 ($\nu = 17-24°$) and was roughly independent of total strain for $\gamma > \approx 0.4$ (Figure 2).

We analyzed data from a second series of experiments in which the plastic strain increment during a given load cycle varied (Figures 3 and 4). As in the previous case load/unload cycles included a significant plastic strain increment for $\gamma < \approx 0.5$. This was followed by a period (A to B in Figures 3 and 4) in which the plastic strain increment was negligible (<0.005) and then by further load cycling with appreciable plastic strain (Figure 3). In order to show the behavior during the period of negligible plastic strain, the data in Figure 3 are plotted vs. time in Figure 4 and a few key points are noted to facilitate comparison.

Prior to the point marked "A" in Figures 3 and 4 the dilatancy rate increased with cycling, but remained $<\tau/\sigma_n$. During the subsequent period of negligible plastic straining the dilatancy rate exceeded τ/σ_n. Successive load cycles from this period show that $d\varepsilon_v^p/d\gamma^p$ exceeded τ/σ_n for a significant strain increment but not at the highest τ/σ_n values (Figure 5). With renewed accumulation of plastic strain $d\varepsilon_v^p/d\gamma^p$ decreased to a value below τ/σ_n (Figure 3). During this period, the decrease in $d\varepsilon_v^p/d\gamma^p$ with cycling was a function of the plastic strain increment $d\gamma^p$. Note that

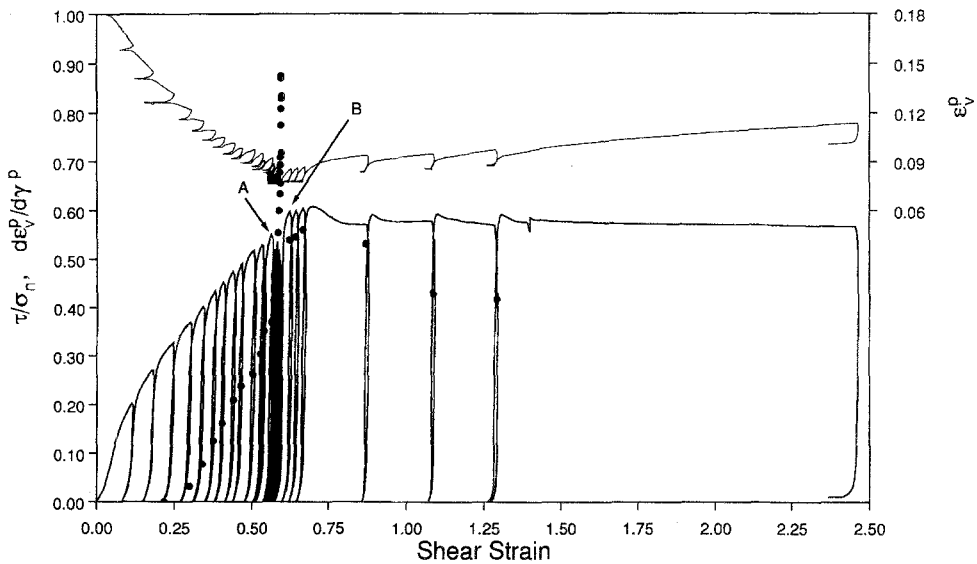

Figure 3

The ratio of shear stress to normal stress τ/σ_n (thick line), plastic volumetric strain ε_v^p (thin line), and the maximum dilatancy rate (dots) are plotted vs. shear strain. Note that $d\varepsilon_v^p/d\gamma^p$ increases sharply, to values above τ/σ_n, during the period of load cycling with negligible plastic strain accumulation (A to B). With renewed plastic straining (after B) $d\varepsilon_v^p/d\gamma^p$ becomes $<\tau/\sigma_n$. During this stage, the reduction in $d\varepsilon_v^p/d\gamma^p$ is proportional to the plastic strain increment. The data of Figure 3 are plotted vs. time in Figure 4 to expand the scale during the many/load/unload cycles from A to B.

the peak stress was highest immediately following the period of cycling load while accumulating negligible plastic strain and that both the peak stress and the shear strain increment between the peak and residual stresses diminished with subsequent plastic straining (Figure 3). In addition, note that load cycling with negligible plastic straining resulted in conpaction and that net dilation occurred during subsequent plastic strain accumulation (Figures 3 and 4).

Discussion and Conclusions

For experiments in which individual load/unload cycles involve appreciable plastic strain (Figures 1 and 2) the data are in accord with the second law, $\sin \nu < \tau/\sigma_n$. The theory also predicts that for a material with cohesion the dilation angle must obey the relation: $\sin \nu \leq \sin \theta + (C/\sigma_n) \cos \theta$, equation (6). To check that it is sufficient to compare the maximum dilation angle with the corresponding friction angle $\theta = \tan^{-1}(\tau/\sigma_n - C/\sigma_n)$ and cohesion term. The mean value of $\nu_{\max}$ is 21° (Figure 2). The mean value of τ/σ_n evaluated at the shear strain at which $\nu_{\max}$ occurs is 0.48 (Figure 2). Using a cohesion of 2.1 MPa (reported by MARONE *et al.*,

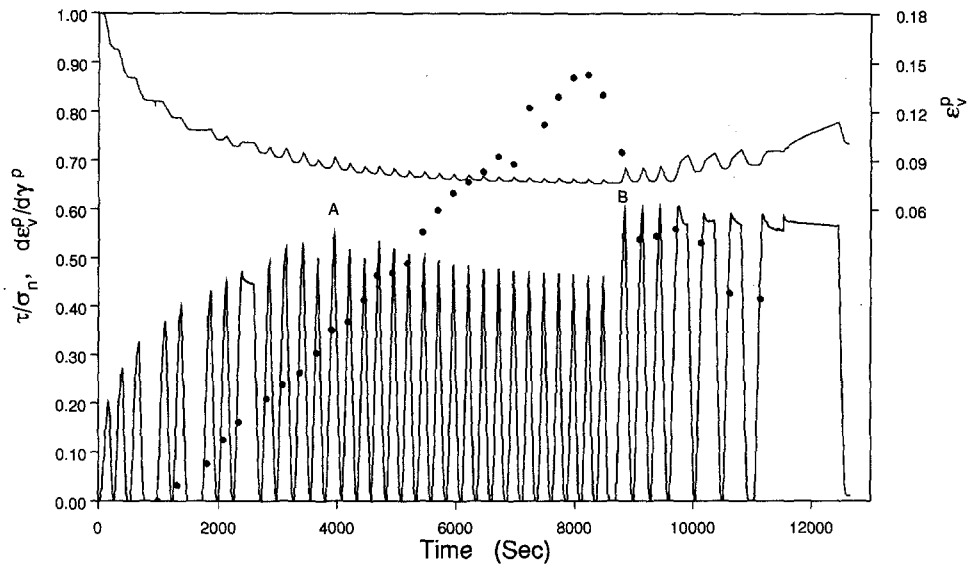

Figure 4

The ratio of shear stress to normal stress τ/σ_n (thick line), plastic volumetric strain ε_v^p (thin line), and the maximum dilatancy rate (dots) are plotted vs. time. These are the same data as shown in Figure 3. $d\varepsilon_v^p/d\gamma^p$ exceeds τ/σ_n during the period of load cycling with negligible plastic strain accumulation (A to B). With renewed plastic straining (after B), $d\varepsilon_v^p/d\gamma^p$ decreases and becomes $<\tau/\sigma_n$.

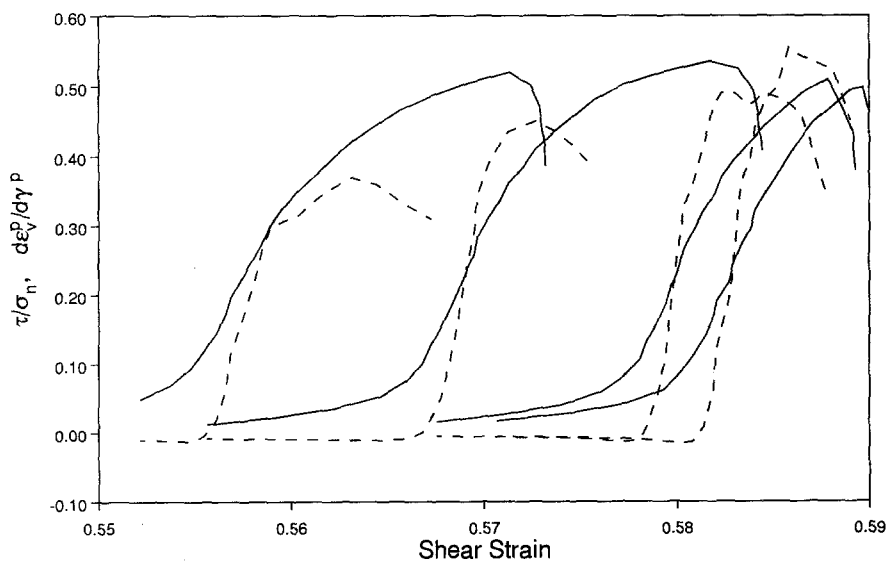

Figure 5

The ratio τ/σ_n (solid line) and dilatancy rate (dashed line) are plotted vs. shear strain for four successive load cycles from the period of negligible plastic strain accumulation in Figures 3 and 4. The dilatancy rate exceeded τ/σ_n for a significant strain increment during loading but did not exceed τ/σ_n at the peak stress. The unloading portion of each curve has been truncated for clarity.

1992, who analyzed data from the same experiments) yields a friction angle of 24.2°. Thus, ν is less than θ in accord with the thermodynamic constraint.

In contrast to these results, load/unload cycles with negligible plastic strain accumulation show $\sin \nu > \tau/\sigma_n$, in violation of equations (6) and (9). This condition is reversible upon further plastic straining (Figure 3). A similar effect is apparent for shear strength: the gouge strengthens during negligible-strain load cycling, as indicated by higher peak stresses during subsequent straining (Figure 3). Both the enhanced peak stress and the large values of $d\varepsilon_v^p/d\gamma^p$ diminish with accumulating plastic strain, indicating a memory effect for past states within the gouge layer. In addition, load cycling without strain accumulation causes compaction that is reversible upon further straining (Figures 3 and 4). The largest net dilation occurs during the first significant increment of plastic strain (third load cycle after the point marked B in Figures 3 and 4).

These effects are indicative of overconsolidation and the accumulation of large residual stresses, which is commonly observed as a result of repeated load/unload cycles (YOUD, 1972). The degree of overconsolidation is clearly extreme in our experiments, perhaps as a result of the high stress state ($50 < \sigma_n < 100$ MPa) and extreme degree of comminution within the gouge. MARONE and SCHOLZ (1989) studied comminution in a similar set of experiments and found (1) that comminution is greatest during the period of strain hardening and net compaction ($\gamma < \approx 1.0$) and (2) that after that point the average particle is less than a few microns in size.

The combination of data showing stress dilatancy relationships in agreement with theory and the reversibility of the condition $d\varepsilon_v^p/d\gamma^p > \tau/\sigma_n$ upon renewed strain accumulation indicates that our results are not a measurement error or an artifact of experimental design. Instead, it seems likely that load cycling with negligible strain enhances grain to grain interlocking producing residual stresses, increased cohesion, and overconsolidation. In this state, shear strain requires rotation between neighboring grains and thus net dilation. The observation that ν exceeds θ and that $d\varepsilon_v^p/d\gamma^p$ exceeds τ/σ_n is presumably the result of dilation associated with residual stress release. Thus, in this sense, the second law constraint is not violated since only the macroscopic stress and strain variables are considered in the simple theory leading to equation (6), and these are not sufficient to fully characterize the thermodynamic state of the deforming system. Evidently, the phenomenon we observe is similar to the Bauschinger effect of metal plasticity.

The loading conditions leading to enhanced cohesion and large dilation angles have an analog in nature: microearthquakes. Microearthquakes on natural faults cause small-amplitude transient loading and this may have an effect on fault gouge similar to that we observed experimentally. Our data indicate that fault gouge will undergo compaction and consolidation during such loading, resulting in a process of *mechanical healing*, which leads to strengthening and changes in the fault zone's

stress-dilatancy relation. Dilatancy may thus be expected on faults with large net offsets, since hundreds or thousands of small amplitude slip events occur for every large (≥ 1 m) slip event. Further, when coupled with the experimental results of MARONE *et al.* (1990) showing a link between dilation and inherently stable frictional behavior our results indicate that in areas where dilation persists over sufficient displacements (on the order of the critical slip distance for seismic faulting) it may tend to inhibit unstable slip.

Acknowledgements

This work derives in part from a series of stimulating conversations with H.-B. Mühlhaus and B. E. Hobbs. I also thank A. Ord for organizing an informative and enjoyable conference on shear localization from which this work benefited. S. J. D. Cox, H.-B. Mühlhaus, and J. W. Rudnicki are thanked for thoughtful reviews.

REFERENCES

DIETRICH, J. H. (1979), *Modeling of Rock Friction: 1. Experimental Results and Constitutive Equations*, J. Geophys. Res. *84*, 2161–2168.

DIETERICH, J. H., *Constitutive properties of faults with simulated gouge*, In *Mechanical Behavior of Crustal Rocks* (eds. Carter, N. L., Friedman, M., Logan, J. M., and Stearns, D. W.) (AGU Monograph 24, 1982) pp. 103–120.

FRANK, F. C. (1965), *On Dilatancy in Relation to Seismic Sources*, Rev. Geophys. *3*, 485–503.

GU, J. C., RICE, J. R., RUINA, A. L., and TSE, S. T. (1984), *Slip Motion and Stability of a Single Degree of Freedom Elastic System with Rate and State Dependent Friction*, J. Mech. Phys. Sol. *32*, 167–196.

HOBBS, B. E., MÜHLHAUS, H.-B., and ORD, A. (1991a), *Instability, softening and localization of deformation*, In *Deformation Mechanisms, Rheology and Tectonics* (eds. Knipe, R. J., and Rutter, E. H.) Spec. Pub. Geol. Soc. London *148*, 143–165.

LAMBE, T. W., and WHITMAN, R. V., *Soil Mechanics* (John Wiley, New York 1969).

MARONE, C., HOBBS, B. E., and ORD, A. (1992), *Coulomb Constitutive Laws for Friction: Contrasts in Frictional Behavior for Distributed and Localized Shear*, submitted to Pure and Appl. Geophys.

MARONE, C., and SCHOLZ, C. H. (1989), *Particle-size Distribution and Microstructures within Simulated Fault Gouge*, J. Struct. Geol. *11*, 799–814.

MARONE, C., RALEIGH, C. B., and SCHOLZ, C. H. (1990), *Frictional Behavior and Constitutive Modeling of Simulated Fault Gouge*, J. Geophys. Res. *95*, 7007–7025.

MEAD, W. J. (1925), *The Geologic Role of Dilatancy*, J. Geol. *33*, 685–698.

ORD., A., VARDOULAKIS, I., and KAJEWSKI, R. (1991), *Shear Band Formation in Gosford Sandstone*, Int. J. Rock Mech. Min. Sci. and Geomech. Abstr. *28*, 397–409.

RUDNICKI, J. W. (1988), *Physical Models of Earthquake Instability and Precursory Processes*, Pure and Appl. Geophys. *126*, 531–554.

RUDNICKI, J. W., and RICE, J. R. (1975), *Conditions for the Localization of Deformation in Pressure-sensitive Dilatant Materials*, J. Mech. Phys. Sol. *23*, 371–394.

RUINA, A. (1983), *Slip Instability and State Variable Friction Laws*, J. Geophys. Res. *88*, 10359–10370.

SCHOLZ, C. H., *The Mechanics of Earthquakes and Faulting* (Cambridge 1990).

SCHOLZ, C. H., SYKES, L. R., and AGGARWAL, Y. P. (1973), *Earthquake Prediction: A Physical Basis*, Science *181*, 803–810.

TULLIS, T. E. (1988), *Rock Friction Constitutive Behavior from Laboratory Experiments and its Implications for an Earthquake Prediction Field Monitoring Program*, Pure and Appl. Geophys. *126*, 555–588.

VERMEER, P. A., and DE BORST, R. (1984), *Non-associated Plasticity for Soils, Concrete and Rock*, Heron *29*, 1–64.

YOUD, T. L. (1972), *Compaction of Sands by Repeated Shear Straining*, J. Soil Mech. and Foundations Div., ASCE *98*, 709–725.

(Received February 17, 1991, accepted November 6, 1991)